Titel/Title: Comprehensive analysis of the thermal impact and its depth effect in grinding

Autor*innen/Author(s): C. Heinzel, J. Heinzel, N. Guba, T. Hüsemann,

Veröffentlichungsversion/Published version: Postprint

Publikationsform/Type of publication: Artikel/Aufsatz

(https://www.sciencedirect.com/science/article/pii/S0007850621000342)
Abstract: The focus of this work is the analysis of the thermal impact and its depth effect in different grinding processes. The investigated processes cover different kinematics and thus broad ranges of the relative speeds and the intensities of the moving heat source regarding the ground surface. A uniform lower process limit characterizing the onset of

Comprehensive analysis of the thermal impact and its depth effect in grinding

Heinzel, C.* (2)[a,b], Heinzel, J.[a,b], Guba, N.[b], Hüsemann, T. [b]

[a] *University of Bremen, MAPEX Center for Materials and Processes, Faculty of Production Engineering, Dept. of Manufacturing Processes, Bremen, Germany*
[b] *Leibniz Institute for Materials Engineering, Dept. of Manufacturing Technologies, Badgasteiner Str. 1-3, D-28359 Bremen, Germany*

The focus of this work is the analysis of the thermal impact and its depth effect in different grinding processes. The investigated processes cover different kinematics and thus broad ranges of the relative speeds and the intensities of the moving heat source regarding the ground surface. A uniform lower process limit characterizing the onset of grinding burn for the different kinematics is identified by means of the specific grinding power and the contact time. The experimental results together with the theoretical considerations of peak temperatures lead to the conclusion that the process specific range of the contact time is mainly responsible for the thermal depth effect. The results enable the targeted exceeding of the critical process limit in roughing and the subsequent correction by finishing.

Grinding, Surface Integrity, Thermal Effect

1. Introduction and state-of-the-art

Grinding processes lead to a thermomechanical load, which influences the surface and subsurface area of workpieces during grinding. The thermal effect on the surface and subsurface layers of steel workpieces is a limiting factor in the design of multi-step grinding processes consisting of roughing and finishing. The roughing step may cause thermal damage (grinding burn) to a certain depth below the surface which may not be removed by the subsequent finishing step, as the stock that is associated with finishing might be smaller than the affected depth from roughing. The thermal effect is due to the generation and distribution of heat to the interacting components, e.g. grinding wheel, fluid, workpiece, involved in the grinding process, which were analysed in detail by Rowe, Jin and Stephenson among others [1, 2, 3]. There is a series of research studies which discuss the so-called grinding burn limit in an experimental [4, 5, 6] as well as in an analytical and modelling way [5, 7]. Pioneering work was done by Malkin et al. [8, 9] based on the moving heat source approach of Carslaw and Jaeger [10]. Malkin et al. assumed that a maximum surface temperature must not be exceeded. Therefore they defined a critical specific energy that in particular depends on the grinding parameters depth of cut a_e and tangential feed rate v_{ft} in conventional surface and external cylindrical plunge grinding [8]. Heinzel et al., on the basis of their own work and the experimental data of Malkin et al., showed that a critical limit can be defined not only based on the specific energy but also taking into account the specific grinding power linked with the contact time (l_g/v_{ft}). This approach can be derived from Malkin's analytical solution [11]. Takazawa also used the considerations of Carslaw and Jaeger and derived an equation for the maximum temperature $T_{max}(Z)$ below the surface [12]:

$$T_{max}(Z) = \frac{2 \cdot q_w}{\rho \cdot c_w \cdot \pi \cdot v_{ft}} \cdot 3.1 \cdot L^{0.53} \cdot e^{-0.69 \cdot Z \cdot L^{-0.37}} \quad (1)$$

In equation (1) q_w denotes the heat flux into the workpiece, c_w the heat capacity, ρ the density of the workpiece material, and Z the dimensionless depth below the surface (equation (2)) and L the dimensionless length of the heat source (equation (3)) according to [12]:

$$Z = \frac{v_{ft} \cdot z}{2\alpha} \quad (2) \qquad L = \frac{v_{ft} \cdot l_g}{2\alpha} \quad (3)$$

In these equations l_g denotes the contact length between wheel and workpiece, z refers to the depth below the surface and α to the thermal diffusivity.

Klocke et al. found - also starting from equation (1) - the favourable influence of high table speeds [13] on the maximum temperature at the surface. In analyses of experimental data from surface grinding tests with conventional grinding wheel, Takazawa took into account not only the maximum temperature below the surface but also explicitly the temporal aspect of heat exposure. He discussed this together with hardness reductions in the surface and subsurface of heat-treated steel workpieces (material: carbon tool steel SK7) resulting from tempering effects by dry and in some cases also by wet grinding. Works by Balart et al. and Jermolajev et al. also show correlations between temperatures, heat exposure times and changes at surface and subsurface [14, 15]. Based on the approach presented in [11], so-called surface layer modification charts for material modifications on the surface were developed [16]. These diagrams show either the surface temperature or the specific grinding power as a function of the contact time and already covered a certain range of medium, conventional grinding parameters. Low specific grinding power together with high contact times, which occur for example in profile grinding, as well as high specific grinding power in combination with very low contact times, as in common generating gear grinding, were not the focus of detailed investigations so far. In particular, the question is still open whether a uniform lower limit for the thermal impact on the surface and subsurface area can be found and which depths of influence are resulting.

2. Research approach

In this paper it is investigated if a uniform process limit for the onset of grinding burn caused by the thermal impact can be found for different kinds of grinding processes. These processes cover various kinematics and thus broad ranges of i) local speeds of the moving heat source on the ground surface as well as ii) specific grinding powers as indicated in Fig. 1. Furthermore, the question

arises whether a similar depth influence due to tempering effects of different kinds of grinding processes can be identified. In order to make corresponding statements as generally valid as possible, the consideration of a certain variety of grinding processes is needed. It has already been discussed in [16] that the contact time, which should be interpreted as the heat impact time of the moving heat source (the grinding wheel) at one point on the generated surface, can differ significantly depending on the kinematics of the grinding process applied. Therefore, three different grinding processes with different engagement kinematics and thus different contact times are chosen.

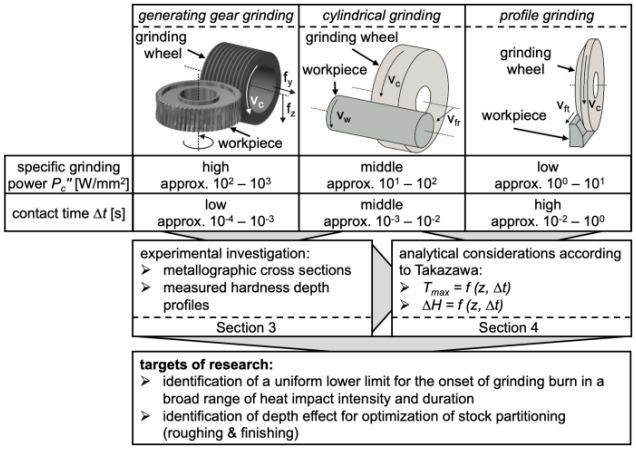

Figure 1. Combined experimental and analytical procedure

Section 3 of this paper focuses on the experimental investigation and evaluation of selected kinematics which differ in their locally applied grinding power and contact times. As part of the experimental procedure data for profile grinding from [16] is used and data for external cylindrical grinding from [17] is re-evaluated with respect to heat impact intensity (specific grinding power P_c'') and impact duration (contact time Δt). In addition, the experimental data is extended into an even shorter contact time regime by considering the continuous generating gear grinding as well. Metallographic micrographs are used to evaluate the respective grinding burn limit and the depth effect of the thermal impact in order to identify a limit of uniform depth influence. The latter aspect is of particular importance for determining the partitioning of stock to be removed by roughing and finishing.

Subsequently, these experimental results are analysed in section 4 by theoretical considerations of the thermal impact in grinding taking into account in particular the impact duration by means of Takazawa's analytical temperature model. On the basis of his experimental results a link between grinding process temperatures, the contact time and the resulting depth-dependent thermal impact on the material can be established. Furthermore, the evaluation of the hardness change of the workpiece and the extrapolation of his findings to shorter and longer contact times enable a comparison between the experimental data of the work presented here and Takazawa's considerations.

3. Experimental results and investigations

To verify the hypothesis that a common thermal limit exists for different grinding processes, the results in [16, 17] from the authors' laboratory are re-evaluated. So far, such considerations have only been carried out for constant or very similar process kinematics. In addition to the results mentioned further findings from continuous generating gear grinding are included. The varied parameters for the experiments and the ground material are summarized in Fig. 2. All other conditions such as the process specific fluid supply strategy (metal working fluid: oil) or conventional grinding wheel specifications were kept constant according to the experimental investigations on a) profile grinding [16], b) external cylindrical grinding [17] and c) roughing by generating gear grinding [18, 19].

profile grinding			***generating gear grinding***		
material stock to be removed	Δs	= 100 – 300 µm	cutting speed	v_c	= 43 – 73 m/s
feed speed	v_{ft}	= 1000 – 6000 mm/min	material stock to be removed	Δs	= 50 – 150 µm
specific material removal rate	Q'_w	= 2 – 30 mm³/(mm·s)	axial feed	f_z	= 0.1 – 1.2 mm/WR
material: AISI1.7147 (case hardened, 57 HRC)			material: AISI1.7131 (case hardened, 61 HRC)		

external cylindrical grinding					
radial feed speed	v_{fr}	= 0.2 – 5.0 mm/min	specific material removal rate	Q'_w	= 1 – 25 mm³/(mm·s)
material: AISI1.6587 (case hardened, 58 HRC)					

Figure 2. Varied process parameters and materials used

In order to ensure a clear assignment of the process forces and the contact time to the respective contact zone during continuous generating gear grinding, these experiments were designed in a contrary way to the typical multi-point contact. There was only a single-point contact between tool and workpiece [19, 20].

In Figure 3, all results obtained from the different grinding processes are shown in a P_c''-Δt-diagram. Green coloured data points symbolize process parameters in which no thermal effect of the machined workpieces was detected. In the case of the red data points, thermal damage was proven by metallographic micrographs showing tempering and in some cases re-hardening zones. The diagram also shows the grinding burn limit according to [11] (dotted line) which is based on Malkin's experimental data [8]. The course of Malkin's grinding burn limit was extrapolated for contact times below 0.001 s and above 0.1 s (indicated by crosses).

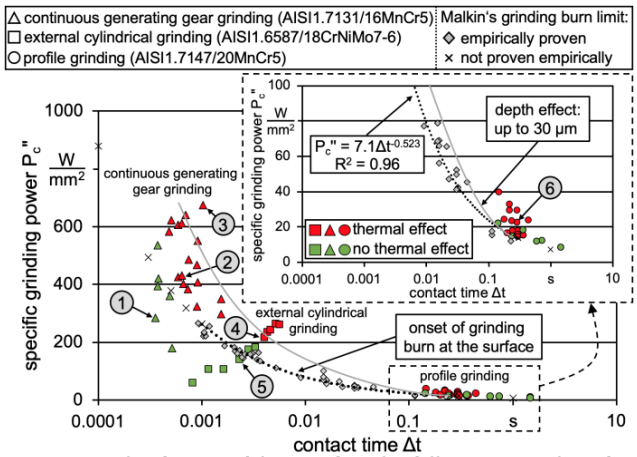

Figure 3. Surface layer modification chart for different types of grinding processes. Experimental points 1-6 refer to exemplary metallographic cross sections in Fig. 4.

Although different system parameters such as grinding wheel specifications and grinding fluids were used, a common thermal lower limit seems to exist for the machined heat treatable steels and the different types of grinding processes. This can be attributed to the fact that the system parameters take effect on the specific grinding power P_c'' and are thus taken into account.

Furthermore, metallographic cross sections were prepared to assess the influenced depth for the different grinding processes. This knowledge is valuable for the optimization of stock partitioning, because the thermally influenced depth does not need to be considered as critical, as far as the stock to be removed in subsequent process steps (e.g. in finishing) is larger than the

affected depth in roughing. It is found that at contact times below 0.001 s (continuous generating gear grinding), even if the thermal damage limit was clearly exceeded, the exemplary micrographs show a thermally affected area region below the surface of lower than 40 µm although temperatures in the contact zone were so high, that in some cases re-hardening zones occurred (point 3 in Fig. 4a and Fig. 3). This is the reason why steep temperature gradients in depth direction are expected in generating gear grinding.

In order to compare the extent of the thermal influence in the depth below the surface for the different grinding processes, exemplary metallographic micrographs of the tempering zones for the different grinding processes are shown in Fig. 4b.

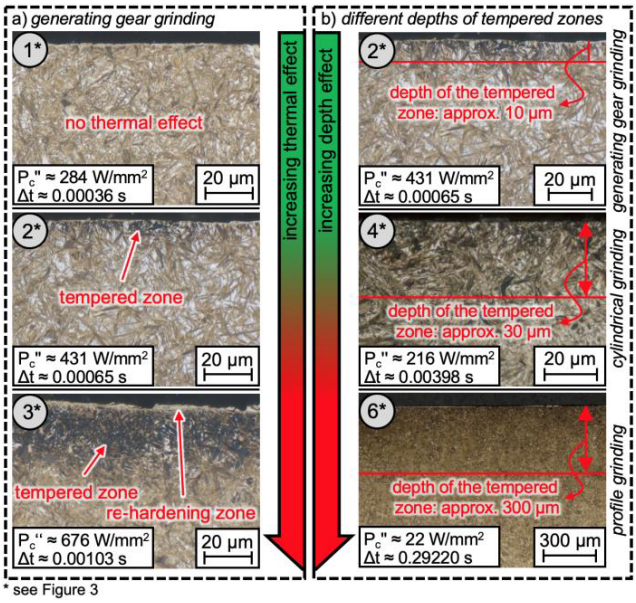

* see Figure 3

Figure 4. a) Increasing depth effect in generating gear grinding and b) Increasing depth effects in different types of grinding processes with different contact times

It can be seen that for contact times above 0.1 s (profile grinding) even a slight excess of the thermal damage limit is sufficient to cause a tempered zone up to a depth of approximately 300 µm (point 6 in Fig. 3). At contact times below 0.1 s, the observed onset of tempering zones with an influenced depth of approximately 30 µm (external cylindrical grinding) or 10 µm (continuous generating gear grinding) is visible despite the fact that the thermal damage limit is clearly exceeded (points 2 and 4 in Fig. 3). In order to illustrate this, a curve is shown in Fig. 3 (in light grey) under which a maximum depth effect of 30 µm was not exceeded based on the experimental data. It can therefore be stated that the depth of the thermally influenced surface layer depends not only on the heat impact intensity but also significantly on the contact time. A strong influence of the contact time on local temperature gradients in depth direction is assumed. The mentioned depth-effect curve illustrates a depth of stock which is plausible to be removed in a finishing grinding process after roughing. For example for external cylindrical grinding, it is found that the specific material removal rate for roughing can be chosen up to three times higher if the depth effect is taken into account for a multi-step grinding process. In comparison to point 4 (Fig. 3), where a specific material removal rate of $Q'_w = 12$ mm³/(mm·s) was chosen and a depth effect below 30 µm was generated, point 5 was realized by a removal rate of only $Q'_w = 4$ mm³/(mm·s) which is closest to the grinding burn limit in the area where no grinding burn was observed. This example illustrates the significance of taking the depth effect into account when determining the partitioning of the stock to be removed in roughing and finishing. This bears the potential of substantial productivity increase.

4. Theoretical considerations

To obtain qualitative statements regarding the local temperature gradients especially in contact time ranges of continuous generating gear and profile grinding experiments, an extrapolation of Takazawa's model is performed.

His model and experimental findings enable a representation of the thermal impact and the depth effect by grinding as well as the resulting material modification in one diagram. For dry surface grinding experiments by Takazawa [12], the hardness was evaluated which resulted at any point beneath the ground workpiece surface with the contact time and peak temperature as parameter. Takazawa's fitted isotherms are used to re-evaluate his experimental results in a surface layer modification chart in Fig. 5.

To achieve this, the following simplifying assumptions and equations are used: a) $q_w = \varepsilon \cdot P_c''$, whereby ε denotes the grinding energy partition ratio according to [9], b) $\rho = 7800$ kg/m³ = const., c) $c_w = 500$ J/(kg·K) = const., d) $\alpha = 13.5$ mm²/s = const. and e) $l_g = \Delta t \cdot v_{ft}$. By inserting a) to e) in equation (1) and considering equation (2) and (3) the resulting functional relationship is derived:

$$\frac{T(z)}{°C} = 133.33 \cdot \varepsilon \cdot \frac{P_c''}{\frac{W}{mm^2}} \cdot \left(\frac{\Delta t}{s}\right)^{0.53} \cdot \left(\frac{v_{ft}}{\frac{m}{s}}\right)^{0.06} \cdot e^{-521.30 \cdot \left(\frac{v_{ft}}{\frac{m}{s}}\right)^{0.26} \cdot \left(\frac{\Delta t}{s}\right)^{-0.37} \cdot \frac{z}{m}} \quad (4)$$

Following this equation the temperature in a certain depth beneath the workpiece surface can be calculated for any contact time. The following Fig. 5 shows the exemplary calculation result for the roughly estimated assumption that $v_{ft} = 6000$ mm/min and that an arbitrary constant peak temperature of 600 °C at the workpiece surface is reached at any contact time. The latter is chosen as in [15] temperatures between 500 °C and 700 °C at the workpiece surface led to the occurrence of tempered zones. The chosen velocity v_{ft} corresponds to an average velocity of the moving heat source in common profile grinding. The moving heat source velocity in external and generating gear grinding is usually larger than this, which would lead to even lower temperatures in certain depths than shown in Fig. 5. So, Figure 5 reveals a worst case estimation for the process kinematics with higher moving heat source velocity.

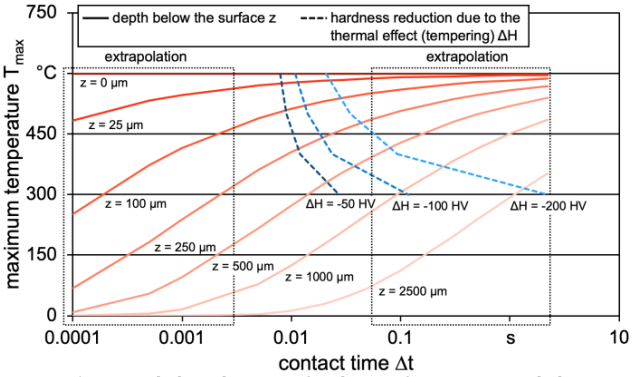

Figure 5. Expanded evaluation of Takazawa's experimental data in a surface layer modification chart

For the mentioned boundary conditions also the change in hardness in comparison to the initial hardness is evaluated from results in [12]. Based on these experimental data from

temperature and hardness measurements after grinding the dashed lines in Fig. 5 were plotted.

As a result of this procedure a modification of the material (hardness reduction ΔH) as a function of local temperature and contact time is shown, which is also referred to as "process signature" [21]. Furthermore, the assumptions and especially the boundary condition T(z=0) = 600 °C reflect the orders of magnitude of the specific grinding powers at the corresponding contact times as indicated in Fig. 1 and as observed in the experimental investigations in section 3. This was verified by using the approach of Malkin for determining the grinding energy partition ratio ε [9].

The middle part of the diagram refers to data from [12]. Furthermore, equation (4) is used for extrapolations of the temperatures in constant depths for higher and lower contact times. Thus qualitative statements can be derived regarding the local temperature gradients in contact time ranges of continuous generating gear grinding and of profile grinding experiments. The lines which represent the temperature in constant depths differ widely in short contact times which correspond to generating gear grinding. This reveals steeper local temperature gradients and thus, a lower depth effect of the thermal impact at these low contact times. This result corresponds to the findings in section 3 with regard to the depth effect in generating gear grinding shown in Fig. 4a). Despite a high heat intensity, represented by P_c'', and the occurrence of re-hardening layers, comparatively low negatively influenced depths (< 30 µm) of the surface and subsurface area of the workpieces are found. For higher contact times the temperatures in a constant depth depending on the contact time converge to the surface temperature. According to this, high temperatures are reached at high depths and lead to high depth effects. This can be exemplarily confirmed by the results from profile grinding, where in fact high depth effects lead to a higher degree of material modification. Corresponding to the experimental point 6 in Fig. 3 and the metallographic cross section no. 6 in Fig. 4 the change of hardness on the workpiece was analysed and amounts to approx. ΔH = 170 HV1 at a point close to the workpiece surface (in a depth of 50 µm). Also the influence on the measured hardness depth profile up to a depth of about 400 µm was observed.

The results obtained by this theoretical consideration are in good agreement with the results of the experimental part in section 3, shown in Fig. 3.

5. Conclusions

A uniform lower process limit for the onset of grinding burn caused by the thermal process impact was identified for different kinds of grinding processes. The investigated grinding processes (generating gear grinding, external cylindrical grinding as well as profile grinding) were chosen, because they differ in particular in their kinematics with regard to duration and intensity of heat impact.

The apparently uniform lower thermal limit is presented in a P_c''-Δt-diagram and can be used to avoid grinding burn indicated in metallographic micrographs. Due to the fact that process kinematics, ground material, applied grinding fluid, grinding wheel and dressing conditions differ, this lower thermal limit seems to cover a wide range of grinding processes. The associated depth effect is mainly influenced by the process specific heat impact duration. The assumption that different local temperature gradients occur at different contact times when the thermal limit is exceeded was confirmed by analysing the experimental results by means of the analytical temperature model according to Takazawa [12]. As the heat dissipation into the grinding fluid and surrounding media is neglected, this analytical approach is used here as a worst-case scenario. The extrapolation towards low contact times reveal that high local temperature gradients are resulting, which lead to a low depth effect (generating gear grinding). Much lower local temperature gradients are resulting as a consequence of high contact times (profile grinding) and can lead to high depth effects of the thermal impact although heat impact intensity is comparably low.

From the authors' point of view, these findings are of high relevance with regard to the process design and optimization as they suggest the targeted exceeding of the critical process limit in roughing and the subsequent correction by finishing. Besides, this knowledge is very valuable for the evaluation of surface and subsurface area states by non-destructive micromagnetic testing and the definition of process kinematic specific grinding burn degrees requested by industry.

Acknowledgements

The scientific work has been supported by the Deutsche Forschungsgemeinschaft (DFG) within the research priority program SPP 2086 (KA 1006/28-1) and also within the collaborative research center SFB/TRR136, sub project F06 (INST 144/361-2). The authors thank the DFG for this funding and support.

References

[1] Rowe W B, Morgan M N, Black S C E, Mills B (1996), A simplified approach to thermal damage in grinding. Annals of the CIRP, 45/1:299-302.
[2] Jamshidi H, Budak E (2018) Grinding Temperature Modelling based on a Time Dependent Heat Source. Procedia CIRP 77:299-302.
[3] Jin Z, Stephenson D (2006) Heat flux distributions and convective heat transfer in deep grinding. Int. Journal for Machine Tools & Manufacture 46:1862-1868.
[4] Denkena B, Jung M, Müller C, Walden L (2003) Charakterisierung weißer Schichten nach mechanischer und thermischer Einwirkung durch Fertigungsverfahren. HTM 58:211-217.
[5] Baumgart C, Heizer V, Wegener K (2018) In-process Workpiece based Temperature Measurement in Cylindrical Grinding. Procedia CIRP 77:42-45.
[6] Aurich J, Kirsch B (2013) Improved Coolant Supply through Slotted Grinding Wheel. Annals of the CIRP 62/1:363-366.
[7] Brinksmeier E, Aurich J, Govekar E, Heinzel C, Hoffmeister H, Klocke F, Peters J, Rentsch R, Stephenson S, Uhlmann E, Weinert K, Wittmann M (2006) Advances in Modeling and Simulation of Grinding Processes. Annals of the CIRP 55/2:667-696.
[8] Malkin S, Lenz E (1978) Burning limit for surface and cylindrical grinding of steels. Annals of the CIRP 27/1:233-236.
[9] Malkin S, Guo C (2007) Thermal Analysis of Grinding. Annals of the CIRP 56/2:760-782.
[10] Carslaw H, Jaeger J C (1959) Conduction of heat in solids, Oxford Science Publications. Oxford University Press.
[11] Heinzel C, Sölter J, Jermolajev S, Kolkwitz, B, Brinksmeier E (2014) A versatile method to determine thermal limits in grinding. Procedia CIRP 13:131-136.
[12] Takazawa K (1966) Effects of grinding variables on surface structure of hardened steel. Bulletin of the Japan Society of Grinding Engineers 2/1:14-21.
[13] Klocke F, Zeppenfeld C, Nachmani Z (2006) Schnellhubschleifen – Mechanische und thermische Energiebilanzen. wt Werkstattstechnik online 96/6:366-371.
[14] Balart M J, Bouzina A, Edwards L, Fitzpatrick M E (2004) The onset of tensile residual stresses in grinding of hardened steels. Materials Science and Engineering A 367:132–142.
[15] Jermolajev S, Brinksmeier E, Heinzel C (2018) Surface layer modification charts for gear grinding. Annals of the CIRP 67/1:333-336.
[16] Guba N, Heinzel J, Heinzel C, Karpuschewski B (2020) Grinding burn limits: Generation of surface layer modification charts for discontinuous profile grinding with analogy trials. CIRP Journal of Manufacturing Science and Technology 31:99-107.
[17] Heinzel J, Sackmann D, Karpuschewski B (2019) Micromagnetic Analysis of Thermally Induced Influences on Surface Integrity Using the Burning Limit Approach. Manuf. Mater. Process. 3/93.
[18] Jermolajev S, Karpuschewski B (2019) Technological limits during continuous generating gear grinding and their link to the preceding workpiece heat treatment, 7th GETPRO International Conference, 19th-20th March 2019, Würzburg (Germany).
[19] Jermolajev S (2020) Thermo-mechanische Prozessgrenzen für das Verzahnungsschleifen. Dr.-Ing. thesis, Universität Bremen.
[20] Dietz C (2017) Numerische Simulation des kontinuierlichen Wälzschleifprozesses unter Berücksichtigung des dynamischen Verhaltens des Systems Maschine – Werkzeug – Werkstück. PhD thesis, ETH Zürich.
[21] Brinksmeier E, Meyer D, Heinzel C, Lübben T, Sölter J, Langenhorst L, Frerichs F, Kämmler J, Kohls E, Kuschel S (2018) Process Signatures - The Missing Link to Predict Surface Integrity in Machining. Procedia CIRP 71:3-10.